Theoretical and experimental analysis of tunable Sagnac high-birefringence loop filter for dual-wavelength laser application

R. I. Álvarez-Tamayo,[1,*] M. Durán-Sánchez,[2] O. Pottiez,[3] E. A. Kuzin,[4] B. Ibarra-Escamilla,[4] and A. Flores-Rosas[4]

[1]Benemérita Universidad Autónoma de Puebla Facultad de Ciencias Fisico-Matematicas, Av. San Claudio y 22 Sur, Puebla, Puebla 72000, Mexico

[2]Universidad Tecnológica de Puebla, Antiguo Camino a la Resurrección 1002-A, Puebla, Puebla. 72000, Mexico

[3]Centro de Investigaciones en Óptica, Loma del Bosque #115 Lomas del Campestre, León, Guanajuato 37150, Mexico

[4]Instituto Nacional de Astrofísica, Óptica y Electrónica, Óptica, Luis Enrique Erro No. 1, Puebla, Puebla 72000, Mexico

*Corresponding author: alvarez.tamayo@hotmail.com

Received 19 August 2010; revised 18 November 2010; accepted 26 November 2010; posted 1 December 2010 (Doc. ID 133589); published 13 January 2011

We present detailed investigations of the spectral dependencies of the transmission of a fiber optical loop mirror (FOLM) consisting of a coupler with output ports spliced at arbitrary angles to a high-birefringence (Hi-Bi) fiber. The application for dual-wavelength lasers is discussed. For this aim, the spectral dependence of the reflection is tuned by the temperature of the Hi-Bi fiber that allows a fine adjustment of the cavity loss for generated wavelengths. The ratio between maximum and minimum reflection can be adjusted by the twist angle of the fiber at the splices, which also provides useful possibilities for the adjustment of cavity losses. We used the twist and temperature variation of the Hi-Bi fiber to change the operation from single wavelength to stable dual-wavelength generation with either equal or unequal powers of wavelengths. © 2011 Optical Society of America

OCIS codes: 060.3510, 260.1440, 060.2420.

1. Introduction

The fiber optical loop mirror (FOLM) with Hi-Bi fiber in the loop has been widely used since its appearance for the implementation of optical devices such as wavelength division multiplexers [1,2], for tuning fiber lasers [3,4], as a spectral filter for switching of multiwavelength fiber lasers [5,6], and for gain flattening and amplified spontaneous emission (ASE) noise elimination in erbium-doped fiber (EDF) amplifiers [7,8]. The FOLM presents considerable advantages, such as low cost, low insertion loss, easy construction. and independence on the input polarization [2,9]. This device consists of a directional coupler with output ports connected to a birefringent fiber. The spectral selectivity of the interferometer is caused by birefringence that has to be introduced to the loop. A lot of effort has been made to suggest and investigate a variety of FOLM designs. Ma *et al.* [10] demonstrated polarization independence of the Hi-Bi FOLM. Mirza and Stewart [11] performed analysis of the FOLM with a rotatable fiber wave retarder for multiwavelength laser application. Liu *et al.* [12] reported a study of an optical filter consisting of two concatenated Hi-Bi FOLMs. Lim *et al.* [13] analyzed the behavior of an FOLM with a fiber loop consisting of two Hi-Bi fibers connected in series. The

0003-6935/11/030253-08$15.00/0

transmittance spectrum of the FOLM presents a periodic behavior with maxima and minima depending on the Hi-Bi fiber length and birefringence. The possibility to tune the wavelengths of maximum transmittance has been reported using different methods, such as the use of polarization controllers in the fiber loop [3,10,13], the use of a small birefringence loop (SBL) to change the orientation of birefringence axes [11], and applying mechanical pressure on a Hi-Bi fiber section [4]. A simple and practical method consists in adjusting the twist of the fiber sections where the low birefringence coupler port is spliced with the Hi-Bi fiber [9,14]. Also, birefringence can be changed through variation of temperature of the Hi-Bi fiber [15], causing by this way a shift of the maxima and minima of transmission. The dependence of birefringence on temperature is approximately a linear dependence [16].

Multiple-wavelength lasers generated interest in recent years because of their potential applications. The generation of multiple wavelengths requires careful adjustment of gain/loss. FOLM-based spectral filters are useful devices for multiple-wavelength fiber lasers due to their large bandwidth, the possibility to control the transmittance spectrum, and their simplicity. Switchable and multiwavelength fiber lasers using an FOLM have been reported [5,17,18]. The FOLM requires an adjustment of polarization in the loop. Usually, polarization controllers are used for this task, but the adjustment is not straightforward. In Ref. [18], the FOLM with temperature adjustment of the reflection spectrum was considered for dual-wavelength laser application and it was shown that this approach provides a straightforward and quantifiable way of adjustment for dual-wavelength operation. However, the FOLM considered in Ref. [14] offers more properties useful for dual-wavelength generation, which had not been discussed before. The twist of the fiber offers a simple way to change the ratio between the maximum and minimum of the reflection in the spectrum dependence (contrast). For spectral filters, the contrast usually has to be as high as possible; however, for dual-wavelength lasers, a low contrast offers the advantage of smoother cavity loss adjustment for the generated wavelengths.

In this paper, we examine numerically and experimentally the variation of the transmission spectrum of an FOLM with the twist of the fiber in the loop. The reflection at the maxima of the spectral dependence of an FOLM including a 3 dB coupler is always 1 (if lossless splices are assumed). The reflection at the minima can be adjusted between 0 and 1 by the twist of the splice segments. This technique provides additional possibilities for applications. The possibility to adjust the contrast is not trivial because the rotation of the splice causes changes of the linear and circular birefringence, both for the coupler port and the Hi-Bi fiber. We have found that residual birefringence causes a shift of the maximum/minimum in the reflection spectrum at the contrast adjustment. This effect is undesirable for dual-wavelength laser applications. However, it was shown that the appropriate choice of the angles of both ends of the Hi-Bi fiber allows contrast variation over a wide range without substantial wavelength shift of the maxima/minima. The rotation of only one of the extremities does not yield the desired result. We demonstrate experimentally the application of the FOLM for dual laser design and compare the laser operation when low contrast and high contrast of transmission spectrum of the FOLM is used. We demonstrate a significant increase of tolerance in dual-wavelength operation with respect to temperature of the Hi-Bi fiber when a low contrast FOLM is used, making smoother the adjustment of losses within the laser cavity. We consider this technique a useful tool for dual-wavelength lasers.

2. Theory

The Hi-Bi FOLM shown in Fig. 1 consists of a fiber coupler with a coupling ratio of $\alpha/1-\alpha$, which is assumed to be independent of wavelength. The output ports (3 and 4) are fusion spliced to a Hi-Bi fiber with arbitrary angles between the axes of the Hi-Bi fiber and the axes of the coupler ports. The segments where the Hi-Bi fiber is spliced to the coupler ports are placed on rotation stages. The Hi-Bi fiber is placed on a thermoelectric cooler to shift the wavelength dependence of the filter transmission. A light beam with electric field E_i enters through port 1; the transmitted beam with electric field E_T exits from port 2.

To calculate the transmission of the FOLM, we used the approach developed by Mortimore [19]. For a single input field E_i, a transmitted field E_T is given by

$$E_T = \begin{pmatrix} E_{Tx} \\ E_{Ty} \end{pmatrix} = \begin{pmatrix} (2\alpha-1)J_{xx} & (1-\alpha)J_{xy}+\alpha J_{yx} \\ -\alpha J_{xy}-(1-\alpha)J_{yx} & (1-2\alpha)J_{xx} \end{pmatrix} \begin{pmatrix} E_{ix} \\ E_{iy} \end{pmatrix}, \quad (1)$$

where the J matrix is calculated as the product of matrices corresponding to all elements in the loop:

$$J = U_1 \cdot C_1 \cdot U_2 \cdot C_2 \cdot U_3, \quad (2)$$

where matrices U_1 and U_3 represent the coupler ports; the matrices C_1 and C_2 represent the coordinate rotation accounting for the angles between the axes of the Hi-Bi fiber and those of the coupler ports at the splices; finally, and the matrix U_2 represents the Hi-Bi fiber.

The matrices U_1, U_2, and U_3 take into account linear birefringence of the fibers and the circular birefringence caused by the fiber twist angle ψ. Each of them takes the following form [20]:

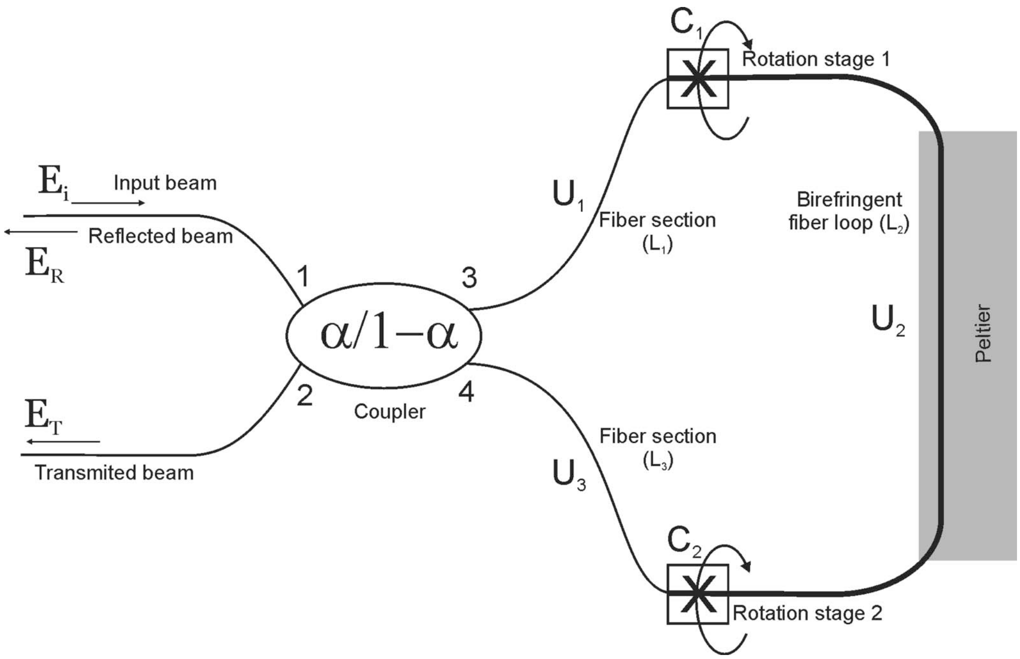

Fig. 1. Schematic of the FOLM with a birefringence fiber in the loop.

$$U_k = \begin{pmatrix} P_k & -Q_k{}^* \\ Q_k & P_k{}^* \end{pmatrix}, \tag{3}$$

where the subscript index k denotes the number of the particular matrix to calculate, being 1 and 3 for the matrices of the coupler ports U_1 and U_3, and 2 for the Hi-Bi fiber, U_2. The elements of the matrices are defined by the following relations:

$$P_k = \cos\eta_k - i\left(\frac{\delta_k}{2}\right)\frac{\sin\eta_k}{\eta_k}, \tag{4}$$

$$Q_k = \left(\psi_k + \frac{\gamma_k}{2}\right)\frac{\sin\eta_k}{\eta_k}, \tag{5}$$

where

$$\eta_k = \sqrt{\left(\frac{\delta_k}{2}\right)^2 + \left(\psi_k + \frac{\gamma_k}{2}\right)^2}. \tag{6}$$

The linear retardance δ_k and circular retardance γ_k are defined as

$$\delta_k = \left(\frac{2\pi}{\lambda}\right)\frac{L_k}{L_{b,k}} \cdot \lambda_0, \tag{7}$$

$$\delta_k = g \cdot \psi_k, \tag{8}$$

where $L_{b,k}$ is the beat length of the respective fiber, L_k is the length of the fiber, and the angle ψ_k is the fiber twist. Coefficient g is equal to −0.16 for silica fibers [21] and is the same for all U_K matrices. The fiber twist is imposed by the rotation of the rotational stages by the angles ϕ_1 and ϕ_2. We take the rotation with the positive sign in the clockwise direction, viewing from the coupler into the loop. A positive angle ϕ_1 causes a positive twist for port 1; however, it causes a negative twist for the Hi-Bi fiber. On the other hand, a positive angle ϕ_2 causes a positive twist of port 2 and negative twist of the Hi-Bi fiber. Hence, $\psi_2 = -(\phi_1 + \phi_2)$ for the matrix U_2, while, for matrices U_1 and U_3, ψ takes values of ϕ_1 and ϕ_2, respectively.

The matrices C_1 and C_2 transform the Jones vectors from the Cartesian system related with the axes of the port to that related with the axes of the Hi-Bi fiber. They are given by [20]

$$C_n = \begin{pmatrix} \cos\theta_n & -\sin\theta_n \\ \sin\theta_n & \cos\theta_n \end{pmatrix}. \tag{9}$$

The subscript index n denotes the number of the particular matrix to calculate, being 1 and 2 for matrices C_1 and C_2, respectively. It is important to note that angles θ_1 and θ_2 in the matrices C_1 and C_2 are unknown in practice; however, they are not changed by the adjustment process. The transmission spectrum is given by the ratio between output and input intensities, which can be expressed as

$$T = \frac{I_{\text{out}}}{I_{\text{in}}} = \frac{|E_T|^2}{|E_i|^2}. \tag{10}$$

It is known that the transmission spectrum of the Hi-Bi FOLM is a periodic function whose period is given by the following expression:

$$\Delta\lambda = \frac{\lambda^2}{B \cdot L}, \tag{11}$$

where B is the fiber loop birefringence, L is the fiber loop length, and λ is the wavelength. The values of the transmission minima are defined by the coupling ratio α and are equal to $(2\alpha - 1)^2$, the transmission maxima, however, depends on the rotation of the rotational stages and can be adjusted in the range between $(2\alpha - 1)^2$ and 1 [14]. The adjustment of the values of the transmission maxima can be useful in particularl for dual-wavelength laser applications. However, the rotation of the rotational stages also moves the wavelengths of the maxima and minima. We investigate in detail the properties of the FOLM using Eqs. (1)–(10).

Figure 2 is a three-dimensional representation that shows the calculated transmission spectrum for several values of angle ϕ_1. We used the coupler ports with a length of 0.5 m and a beat length of 6 m. The length of the Hi-Bi fiber is equal to 28 cm with a beat length of 3.6×10^{-3} m. The parameters used in calculations correspond to our experimental setup. The angles $\theta_1 = 0.5\pi$ and $\theta_2 = 0.3\pi$ were taken arbitrarily. To obtain the transmission maximum equal to 1, an adjustment of the angles ϕ_1 and ϕ_2 has to be done. For our case, an angle ϕ_2 equal to -0.8π provides the required adjustment. We can see that the transmission maximum depends on the angle ϕ_1 with a period equal to 1.087π. Figure 3 shows transmission spectra for several values of the angle ϕ_1 taken in the range between 0 and 1.087π. Here we can see that the adjustment of the transmission maximum by changing the angle ϕ_1 also causes a shift of the wavelengths of the maxima.

The wavelength shift of the maximum depends on the birefringence of the coupler ports. Figure 4 shows the wavelength as the angle ϕ_1 is varied for different beat lengths of the coupler ports. Other parameters are the same as for Figs. 2 and 3. As it can be noted, there is a range of the angle ϕ_1 approximately between 0.2π and 0.8π where the wavelength shift is less than 1 nm. The wavelength shift is more pronounced for larger birefringence of the coupler ports.

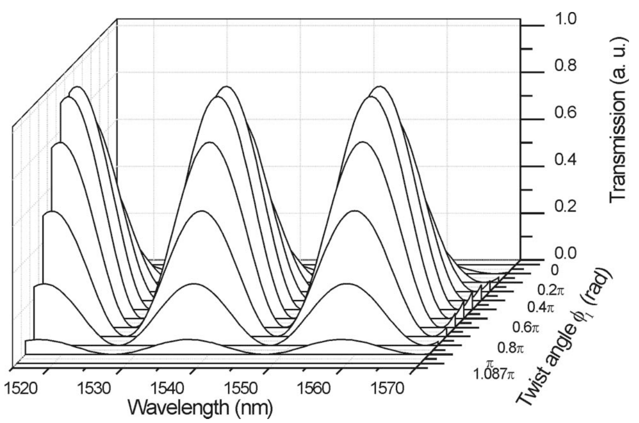

Fig. 2. FOLM transmission as a function of the angle ϕ_1 with fixed ϕ_2.

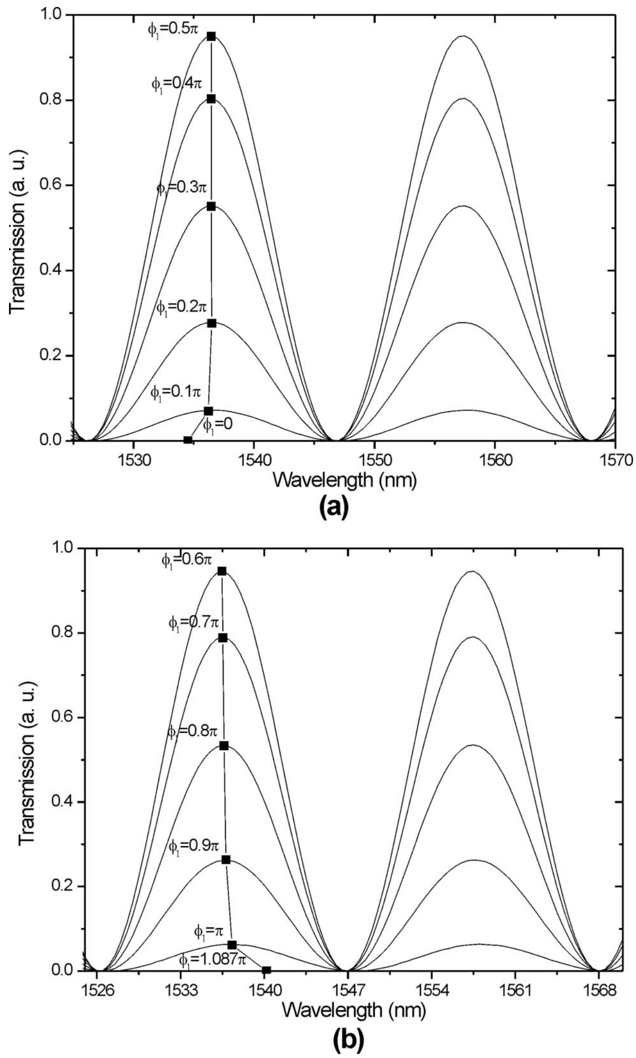

Fig. 3. FOLM transmission spectra as a function of angle ϕ_1 with fixed ϕ_2. (a) Rotation for ϕ_1 from 0 to 0.5π, (b) rotation for ϕ_1 from 0.6π to 1.087π.

3. Experimental Results

We investigated experimentally the Hi-Bi FOLM and a dual-wavelength laser using the scheme shown in Fig. 5. The linear laser cavity is formed by fiber Bragg gratings FBG1 and FBG2 on one side, and the Hi-Bi FOLM at the opposite side of the cavity. The FBG1 has 55.4% maximum reflection at 1548 nm; this wavelength is referred to as λ_1. The FBG2 has 59.75% maximum reflection at 1547 nm; this wavelength is referred as λ_2. As an optical attenuator (OA), we use six turns of the fiber wound on a cylinder with 2.5 cm diameter. The number of turns was found experimentally to equalize roughly the cavity loss for the wavelengths corresponding to the FBGs' maxima. The Hi-Bi FOLM consists of a 50/50 coupler with output ports spliced to a 28 cm Hi-Bi fiber with birefringence $B = 4.22 \times 10^{-4}$. The splices were placed into rotation stages to adjust the transmission of the FOLM. The Hi-Bi fiber temperature is controlled by temperature controller with a precision of 0.1 °C for the purpose of tuning the wavelength of

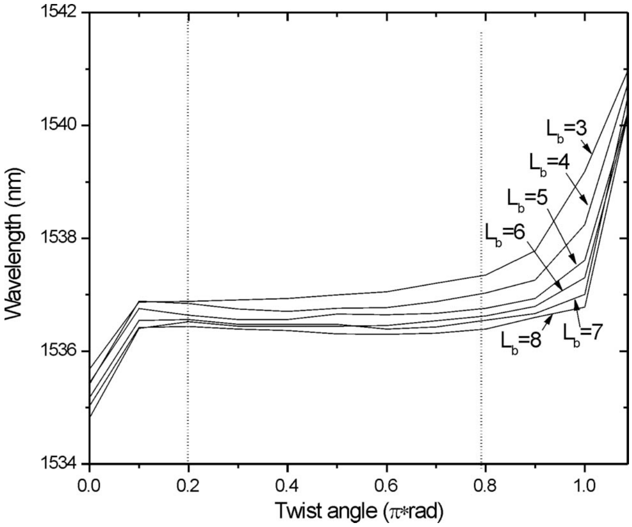

Fig. 4. Dependence of the wavelength shift of the transmission maximum on the angle ϕ_1 for different beat lengths L_b.

the transmission spectra. Temperature can be adjusted in the range between 9 °C and 35 °C. For pumping, we used a 980 nm laser diode with a maximum power of 60 mW. It pumps a 10 m EDF through a 980/1550 wavelength division multiplexer (WDM). The output radiation was launched to a monochromator with a resolution of 0.1 nm, detected by a photodetector, and monitored on an oscilloscope. For measurement of the transmission spectra of the Hi-Bi FOLM, the part of the cavity with the FBGs and the OA was cut and the pump power was decreased below the threshold to avoid lasing (about 25 mW). In this case, the EDF was used as a broadband ASE source.

Figure 6 shows the output spectrum of the FOLM using the EDF with a pump power of 25 mW without FBGs. The measurement was performed at the Hi-Bi fiber temperature of 22.7 °C. To make measurements, we first adjusted the angles of the rotation stages to obtain the transmission very close to 0

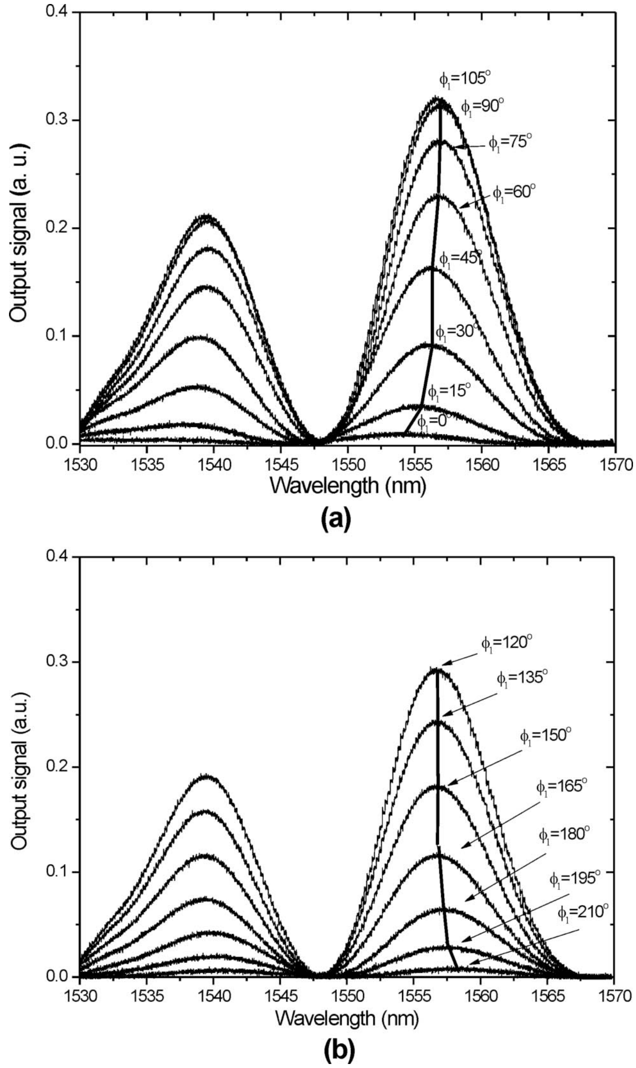

Fig. 6. Spectrum at the FOLM output for different angles ϕ_1 with fixed ϕ_2. (a) Rotation of ϕ_1 from 0° to 105°, (b) rotation for ϕ_1 from 120° to 210°.

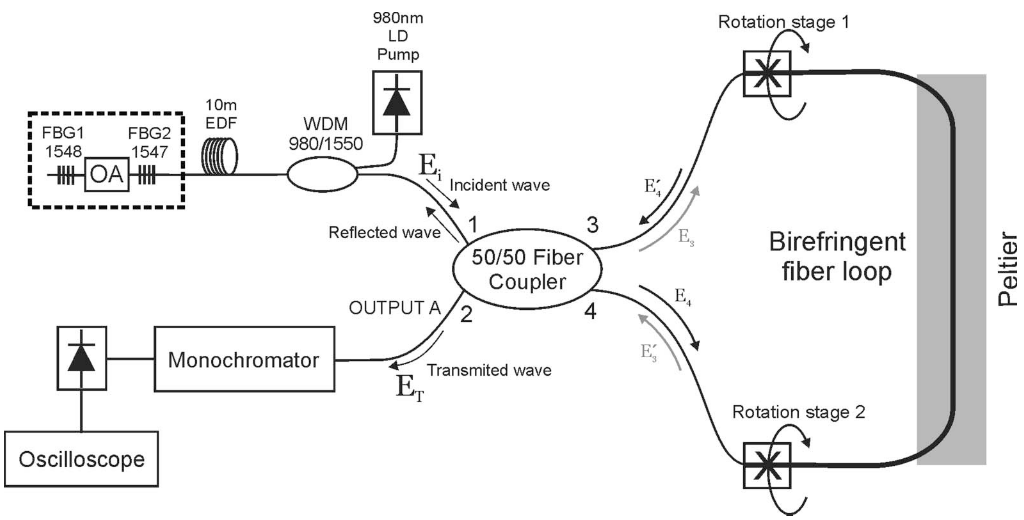

Fig. 5. Schematic diagram of the dual-wavelength laser.

for all wavelengths, the dependence of $\phi_1 = 0$ in Fig. 6(a). At this position, the angle ϕ_2 is fixed and the angle ϕ_1 was referred as 0. Figure 6(a) shows the transmission spectra of the FOLM for the angle ϕ_1 in the range between 0 and 105°; Fig. 6(b) shows the transmission spectra of the FOLM for the angle ϕ_1 in the range between 120° and 210°. Another minimum transmission spectrum was measured at the angle ϕ_1 equal to 1.17π (210°), a value slightly higher than the period found in simulations. The FOLM transmission presents a periodic wavelength dependence with a period of 20.8 nm. It can be seen that the position of the maximum is shifted when the angle ϕ_1 is changed. The maximum is connected by a solid line in Figs. 6(a) and 6(b). However, the period remains the same.

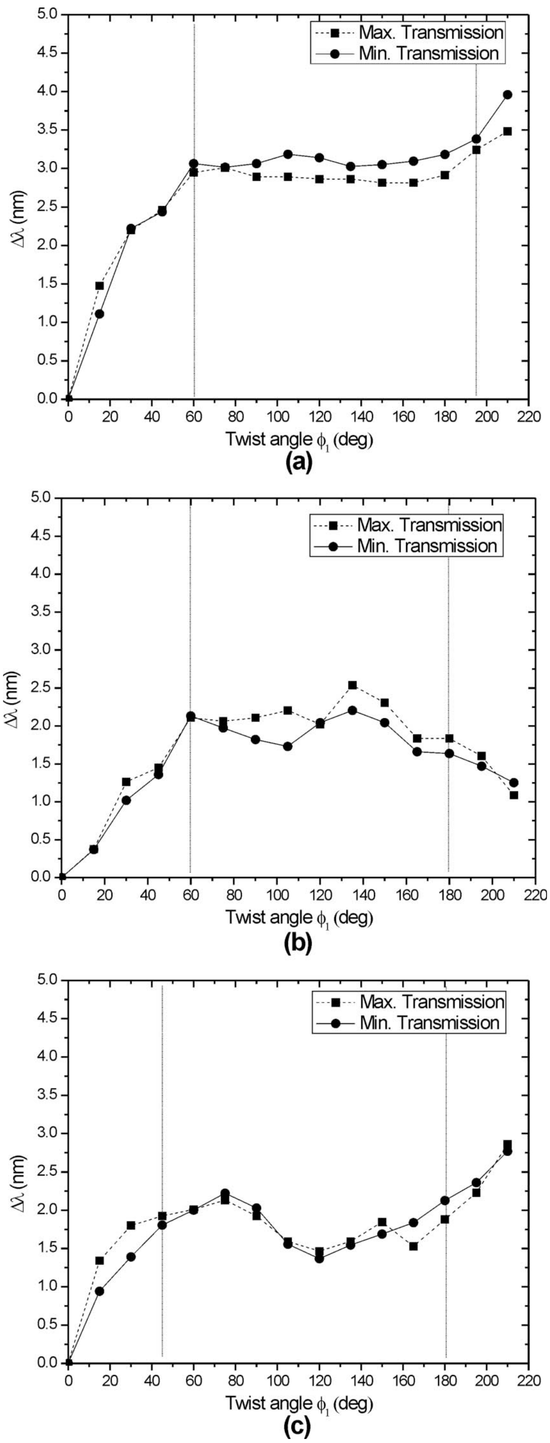

Fig. 7. Dependence of wavelength shift of the transmission maximum and minimum on the angle ϕ_1. (a) $\phi_2 = 55°$, (b) $\phi_2 = 120°$, (c) $\phi_2 = 150°$.

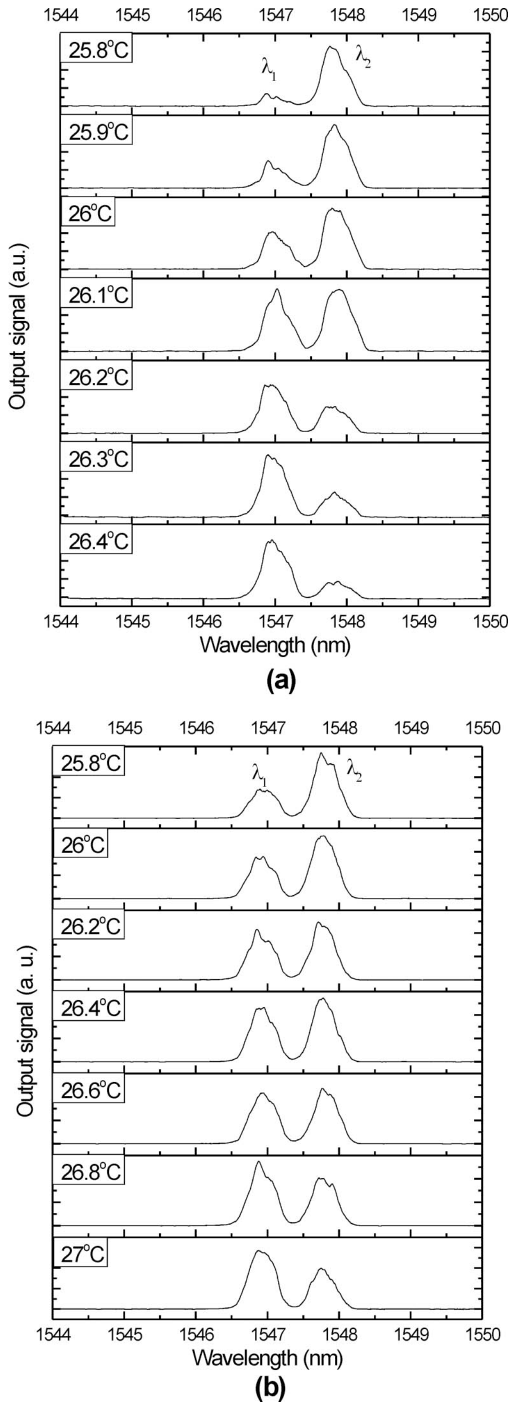

Fig. 8. Laser output spectra at different temperatures. (a) The FOLM spectrum was adjusted to have the highest contrast between the reflection maximum and minimum, $\phi_1 = 120°$. (b) The FOLM spectrum was adjusted to have a low contrast, $\phi_1 = 30°$.

Figure 7 shows the wavelength shift of the maximum and the minimum of transmission due to the variation of the ϕ_1 angle for three different adjustments of the angle ϕ_2. In all cases, the angle ϕ_1 was referred as 0 in the same manner as for Fig. 6(a). The experimental dependences show a behavior similar to that obtained in simulations; see Fig. 4. It can be seen that there exists a range of the angle from about 60° to 180° where the dependence of the wavelength shift is almost flat with variations of less than 0.5 nm (corresponding to only a few percent of the transmission period).

We used the FOLM to adjust the loss of the cavity for wavelengths λ_1 and λ_2 corresponding to the FBG1 and FBG2 to obtain dual-wavelength operation. The idea of the application of the FOLM for dual-wavelength lasers was reported for the first time in Ref. [18]. Here we show the usefulness of the adjustment of the values of the reflection maxima by tuning the angles of the rotation stages. Figure 8 presents the laser spectrum for different temperatures of the Hi-Bi fiber. The temperature of the Hi-Bi fiber was chosen to have a maximum of reflection of the FOLM close to the wavelengths of maximal reflection of the FBGs. A change of the temperature moves the maxima of FOLM transmission and so changes the ratio between the reflections for λ_1 and λ_2. The dependence of the wavelength shift on temperature can be fitted by a linear dependence with a slope of −1.71 nm/°C [18]. The results of Fig. 8(a) are obtained with the FOLM at high contrast between maxima and minima of reflection, while the results of Fig. 8(b) are obtained with low contrast. The change of contrast is achieved through a rotation of the rotational stages, as shown in Fig. 6. In the last case, the dependence of the reflection on the temperature is slower. It can be seen that the range of temperatures over which dual-wavelength generation is observed is larger for Fig. 8(b), providing higher tolerance with respect to the temperature stability. Figure 9 shows the measured power of the two laser lines for the same FOLM adjustment as for Figs. 8(a) and 8(b). Insets in the figures show reflection of the FOLM used for each measurement. We can see that the temperature tolerance of the dual-wavelength operation for the case shown in Fig. 9(b) is much higher than the temperature tolerance for the case shown in Fig. 9(a).

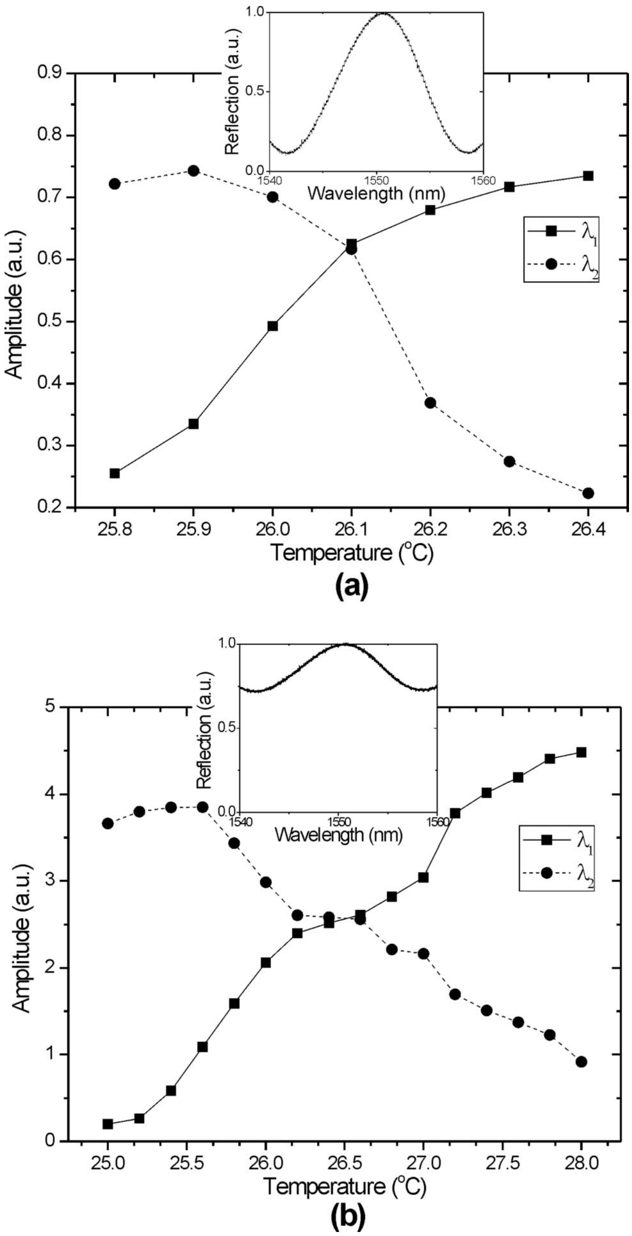

Fig. 9. Power at wavelengths λ_1 and λ_2. (a) Highest contrast between reflection maxima and minima, (b) low contrast between reflection maxima and minima.

4. Conclusions

We report the numerical and experimental analysis of variation in transmission spectrum with a twist of the fiber in the loop of a FOLM used as a spectral filter in a dual-wavelength laser application. The FOLM includes a Hi-Bi fiber spliced with the output of a 50/50 coupler with arbitrary relative orientation of the birefringence axes. The twist of the fiber offers a simple way to change the ratio between the reflection maximum and minimum that provides a useful and simple method for the FOLM contrast adjustment. We found that this contrast adjustment causes a shift of the maximum/minimum in the reflection spectrum that is undesirable for dual-wavelength laser applications. However, the appropriate choice of the angles of both ends of the Hi-Bi fiber allows a reflection minimum between 0 and 0.9 without substantial wavelength shift. The reflection maximum is always equal to 1. For dual-wavelength lasers, low contrast offers the advantage of smoother cavity loss adjustment for the generated wavelengths where the principal mechanism of the adjustment of the cavity loss is the shift of the wavelength of the reflection maxima of the FOLM. The wavelength shift is achieved by the change of the temperature of the Hi-Bi fiber. We were able to generate two wavelengths with a well-controlled ratio between their powers.

B. Ibarra-Escamilla was supported by Consejo Nacional de Ciencia y Tecnologia grant 104551.

References

1. X. Fang and R. O. Claus, "Polarization-independent all-fiber wavelength-division multiplexer based on a Sagnac interferometer," Opt. Lett. **20**, 2146–2148 (1995).
2. A. N. Starodumov, L. A. Zenteno, D. Monzon, and A. R. Boyain, "All-fiber polarization-independent narrow band wavelength-division multiplexer," Opt. Commun. **138**, 31–34 (1997).
3. I. Huixtlaca, G. Beltrán, J. Castillo, and S. Muñoz, "Fiber laser thermally tunable by a filter composed of two Sagnac interferometers," IEEE J. Quantum Electron. **44**, 49–55 (2008).
4. A. Gonzalez, O. Pottiez, R. Grajales, B. Ibarra, and E. A. Kuzin, "Switchable and tuneable multi-wavelength Er-doped fibre ring laser using Sagnac filters," Laser Phys. **20**, 720–725 (2010).
5. S. Hu, L. Zhan, Y. J. Song, W. Li, S. Y. Luo, and Y. X. Xia, "Switchable multiwavelength erbium-doped fiber ring laser with a multisection high-birefringence fiber loop mirror," IEEE Photon. Technol. Lett. **17**, 1387–1389 (2005).
6. S. Feng, O. Xu, S. Lu, X. Mao, T. Ning, and S. Jian, "Switchable dual-wavelength erbium-doped fiber-ring laser based on one polarization maintaining fiber Bragg grating in a Sagnac loop interferometer," Opt. Laser Technol. **41**, 264–267 (2009).
7. S. Li, K. S. Chiang, and W. A. Gambling, "Gain flattening of an erbium-doped fiber amplifier using a high-birefringence fiber loop mirror," IEEE Photon. Technol. Lett. **13**, 1076 (2001).
8. A. Flores-Rosas, E. A. Kuzin, B. Ibarra-Escamilla, and M. Bello-Jiménez, "Eliminación de ruido de ASE en una fibra dopada con erbio empleando un filtro basado en el interferómetro de Sagnac con fibra de Hi-Bi en el lazo," Rev. Mex. Fis. **54**, 130–134 (2008).
9. J. M. Estudillo-Ayala, E. A. Kuzin, and B. Ibarra-Escamilla, "Teoría del interferómetro de Sagnac de fibra de baja birrefringencia y torcida," Rev. Mex. Fis. **47**, 271–274 (2001).
10. X. Ma, G. Kai, and Z. Wu, "Study of polarization independence for high birefringence fiber Sagnac interferometers," Microw. Opt. Technol. Lett. **46**, 183–185 (2005).
11. M. A. Mirza and G. Stewart, "Theory and design of a simple tunable Sagnac loop filter for multiwavelength fiber lasers," Appl. Opt. **47**, 5242–5252 (2008).
12. L. Liu, Q. Zhao, G. Zhou, H. Zhang, S. Chen, L. Zhao, Y. Yao, P. Guo, and X. Dong, "Study on an optical filter constituted by concatenated Hi-Bi fiber loop mirrors," Microw. Opt. Technol. Lett. **43**, 23–26 (2004).
13. K. S. Lim, C. H. Pua, N. A. Awang, S. W. Harun, and H. Ahmad, "Fiber loop mirror filter with two-stage high birefringence fibers," Prog. Electromag. Res. C **9**, 101–108 (2009).
14. E. A. Kuzin, H. Cerecedo-Nuñez, and N. Korneev, "Alignment of a birefringent fiber Sagnac interferometer by fiber twist," Opt. Commun. **160**, 37–41 (1999).
15. W. Eickhoff, "Temperature sensing by mode-mode interference in birefringent optical fibers," Opt. Lett. **6**, 204–206 (1981).
16. K. S. Lim, C. H. Pua, S. W. Harun, and H. Ahmad, "Temperature-sensitive dual-segment polarization maintaining fiber Sagnac loop mirror," Opt. Laser Technol. **42**, 377–381 (2010).
17. X.-J. Jia, Y.-G. Liu, L.-B. Si, Z.-C. Guo, S.-G. Fu, G.-Y. Kai, and X.-Y. Dong, "A tunable narrow-line-width multi-wavelength Er-doped fiber laser based on a high birefringence fiber ring mirror and an auto-tracking filter," Opt. Commun. **281**, 90–93 (2008).
18. M. Durán-Sánchez, A. Flores-Rosas, R. I. Alvarez-Tamayo, E. A. Kuzin, O. Pottiez, M. Bello-Jimenez, and B. Ibarra-Escamilla, "Fine adjustment of cavity loss by Sagnac loop for a dual wavelength generation," Laser Phys. **20**, 1270–1273 (2010).
19. D. B. Mortimore, "Fiber loop reflectors," J. Lightwave Technol. **6**, 1217–1224 (1988).
20. C. Tsao, *Optical Fiber Waveguide Analysis* (Oxford Science, 1992).
21. P. McIntyre and A. W. Snyder, "Light propagation in twisted anisotropic media: application to photoreceptors," J. Opt. Soc. Am. **68**, 149–157 (1978).